Structure and Solvation of Mercury(II) Iodide and Bromide in Tetrahydrothiophene Solution

Magnus Sandström *
Department of Inorganic Chemistry, The Royal Institute of Technology, S-100 44 Stockholm, Sweden
Ingmar Persson
Inorganic Chemistry 1, Chemical Center, University of Lund, P.O. Box 124, S-221 00 Lund, Sweden
Peter L. Goggin
Department of Inorganic Chemistry, The University, Bristol BS8 1TS

The structure of the solvated neutral HgI_2 and $HgBr_2$ molecular complexes in tetrahydrothiophene (tht) solution has been studied by *X*-ray diffraction and vibrational spectroscopic methods. Pseudo-tetrahedral $[HgI_2(tht)_2]$ and $[HgBr_2(tht)_2]$ species of approximately C_{2v} symmetry are formed in solution. The Hg–I bond length is 2.670(4) Å and the Hg–Br 2.535(6) Å. The IHgI angle was found to be 143(2)° at 25 °C and BrHgBr 132(2)° at 30 °C including estimated corrections for shrinkage effects. Raman and i.r. spectra of the solutions and the solids are consistent with molecular models derived from the diffraction data. A comparison with crystal structure data for $[HgBr_2(tht)_2]$ and $[HgCl_2(tht)_2]$ is made.

As part of a series of *X*-ray diffraction and vibrational spectroscopic studies on the solvation of mercury(II) halides in solution and crystals,[1–4] the present paper reports a structural investigation on solutions of HgI_2 and $HgBr_2$ in tetrahydrothiophene (tht), C_4H_8S. The aim of these studies is to correlate the structural changes of the HgX_2 entity with the co-ordinating properties of the solvents, and to serve as a basis for a relative comparison of the donor strengths of a wide range of solvents as probed by the shift in the stretching frequencies of the HgX_2 unit.[1] Previous *X*-ray diffraction studies of HgX_2 solutions have been made with the O-donor solvents dimethyl sulphoxide (dmso) and methanol[3,5] and the N-donor pyridine.[2] The solvent tht, a cyclic thioether, was chosen as a representative for S-donors. The solubilities of HgI_2 and $HgBr_2$ are sufficient for *X*-ray diffraction studies, *ca.* 0.85 and *ca.* 0.65 mol dm^{-3} at 25 °C, respectively, but that of $HgCl_2$ is too low (0.37 mol dm^{-3}).[6] In order to provide a basis for the models of the solvated complexes in solution, the crystal structures of the isomorphous compounds $[HgBr_2(tht)_2]$ and $[HgCl_2(tht)_2]$ were determined and will be reported separately.[4]

Experimental

Preparation of Samples.—Weighed amounts of mercury(II) bromide and iodide, recrystallized from alcohol and acetone, respectively, were dissolved in tht (Fluka). The solvent was distilled (b.p. 120 °C) prior to use. The compositions of the solutions studied are given in Table 1. After some time at 25 °C, crystals were formed in the 0.7 mol dm^{-3} $HgBr_2$ solution, and therefore its temperature was increased to 30 °C. Two mercury(II) iodide solutions were investigated, one at 25 °C and another at 30 °C.

Solution X-Ray Diffractometry.—A large-angle theta–theta diffractometer, previously described,[7] was used to measure the *X*-ray scattering (Mo-K_α, λ = 0.7107 Å) from the surface of the tht solutions. The iodide (30 °C) and bromide solutions were enclosed in a thin-walled (0.15 mm) half-filled cylindrical glass vessel, previously described and calibrated.[2] All data from the iodide solution at 25 °C and low-angle data ($\theta < 10°$) for the other two solutions were obtained using a Teflon cup for the solutions inside a closed cylinder equipped with an aluminium-foil window.

Table 1. Composition of the investigated solutions at the temperature of measurement. The density is denoted ρ and the linear absorption coefficient for Mo-K_α radiation as μ

	X		
	I (30 °C)	I (25 °C)	Br (30 °C)
$[HgX_2]$/mol dm^{-3}	0.724	0.833	0.724
$[C_4H_8S]$/mol dm^{-3}	10.66	10.61	10.8
ρ/g cm^{-3}	1.269	1.319	1.216
μ/cm^{-1}	26.9	30.4	29.0

The scattered intensity was measured repeatedly at discrete points between θ = 1.5 and 70°, where 2θ is the scattering angle. Intervals of 0.1° for $1.5 < \theta < 15°$ and 0.25° for $15 < \theta < 70°$ were used. At least 10^5 counts were accumulated for each point, which corresponds to a statistical error of about 0.3%. The data reduction was performed as described previously[8] by means of the computer program KURVLR.[9] For the normalization of the experimental intensities, a stoicheiometric volume *V*, corresponding to one mercury atom, was chosen. The reduced intensities, $i(s)$, obtained after subtraction of the calculated structure-independent scattering, and multiplied by the scattering variable $s = (4\pi/\lambda)\sin\theta$, are shown in Figure 1. The differential radial distribution functions (r.d.f.s), solid lines in Figure 2(*a*), were obtained from expression (1) in the same way

$$D(r) - 4\pi r^2\rho_0 = (2r/\pi)\int_0^{s_{max.}} si(s)\cdot M(s)\sin(rs)ds \quad (1)$$

as described for pyridine solutions.[2] The modification function used was $M(s) = e^{-0.008s^2}[\Sigma_i f_i(0)]^2/[\Sigma_i f_i(s)]^2$, which sharpens the peaks in the r.d.f.s considerably with an even smaller damping of the oscillations of $i(s)$ at $s_{max.}$ than that used for the pyridine solutions, in order to obtain the highest resolution possible without introducing too much distortion in the r.d.f.s. This was found necessary because the interpretation of the scattering data was based mainly on the fitting of calculated peak shapes to the r.d.f.s.

Table 2. Parameters[a] used for the calculation of model functions for intramolecular interactions of the molecular $[HgX_2(tht)_2]$ complexes in tht solution, with estimated standard deviations for refined parameters in parentheses. Corresponding mean distances without corrections for thermal motion from the crystal structures are given in the last two columns. The internal distances within the tht molecules were also included in the calculations using mean values from the crystal structures

		Solutions			Crystal structures	
Parameter		I (30 °C)	I (25 °C)	Br (30 °C)	$[HgBr_2(tht)_2]$	$[HgCl_2(tht)_2]$
Hg–X	*d*	2.670(4)	2.670(4)	2.535(6)	2.553	2.459
	l	0.073(4)	0.069(4)	0.086(6)		
	n	2.0(1)	2.0(1)	2.0(1)	2	2
X···X	*d*	5.06(2)	5.02(2)	4.60(4)	4.37	4.16
	l	0.16(2)	0.17(2)	0.16(2)		
	n	*n*(Hg–I)/2	*n*(Hg–I)/2	*n*(Hg–Br)/2	1	1
X···S	*d*	4.25(3)	4.25(3)	4.07(4)	4.16	4.06
	l	0.21	0.18	0.17		
	n	4	4	4	4	4
Hg–S	*d*	2.72	2.72	2.62	2.60	2.57
	l	0.14	0.14	0.20		
	n	2	2	2	2	2
Hg···C	*d*	3.50	3.50	3.50	3.50	3.50
	l	0.20	0.20	0.22		
	n	4	4	4	4	4
Hg···C	*d*	3.90	3.90	3.90	4.00	3.97
	l	0.20	0.20	0.24		
	n	4	4	4	4	4
S···S	*d*	4.10	4.10	4.20	4.22	4.20
	l	0.20	0.20	0.25		
	n	1	1	1	1	1
Angle XHgX/°		143(2) 146[b]	140(2) 143[b]	130(3) 132[b]	117.5	115.4

[a] *d* = Distance in Å, *l* = root-mean-square variation in the distance (the temperature coefficient, $b = l^2/2$), and *n* = frequency of the distance. [b] With estimated correction for shrinkage, see text.

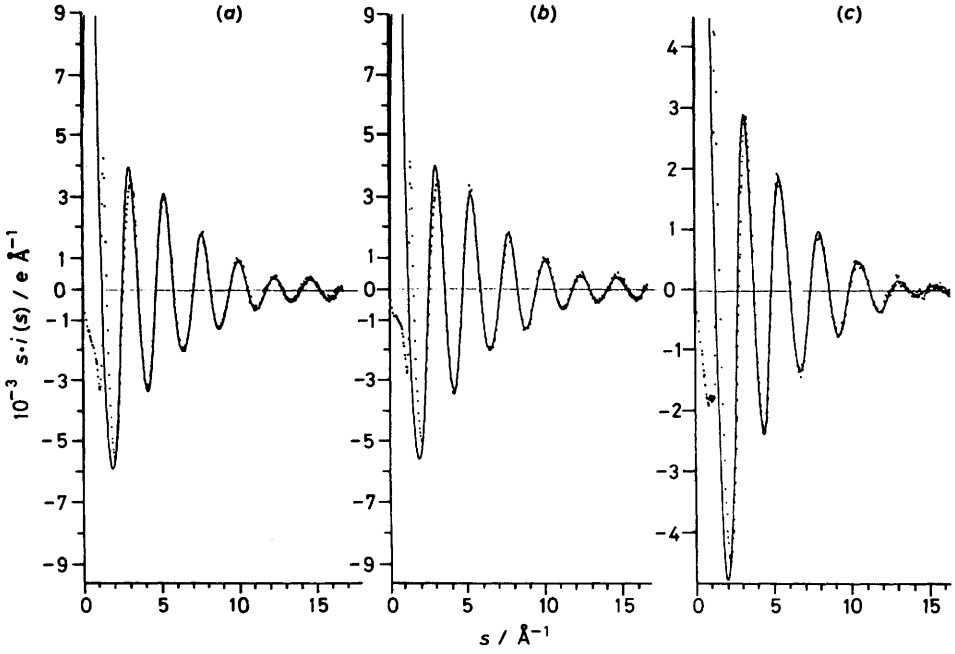

Figure 1. Experimental (dots) and calculated (solid lines) reduced intensity curves *i*(*s*) multiplied by *s* for thf solutions of (*a*) HgI_2 (30 °C), (*b*) HgI_2 (25 °C), and (*c*) $HgBr_2$ (30 °C). The parameters given in Table 2 were used for calculation of the model curves for the molecular complexes $[HgX_2(tht)_2]$

Vibrational Spectra.—Far-i.r. spectra were measured with a Nicolet 7199A Fourier-transform system with a 6.25-μm Mylar beamsplitter, Globar source, and a deuteriated triglycine sulphate detector with polyethylene windows. Solutions in tht were contained in cells with high-density polyethylene windows and sample thicknesses of 0.5 mm. Solids were measured as mulls in petroleum jelly to which a trace of tht had been added; in each case, duplicate successive measurements were made to

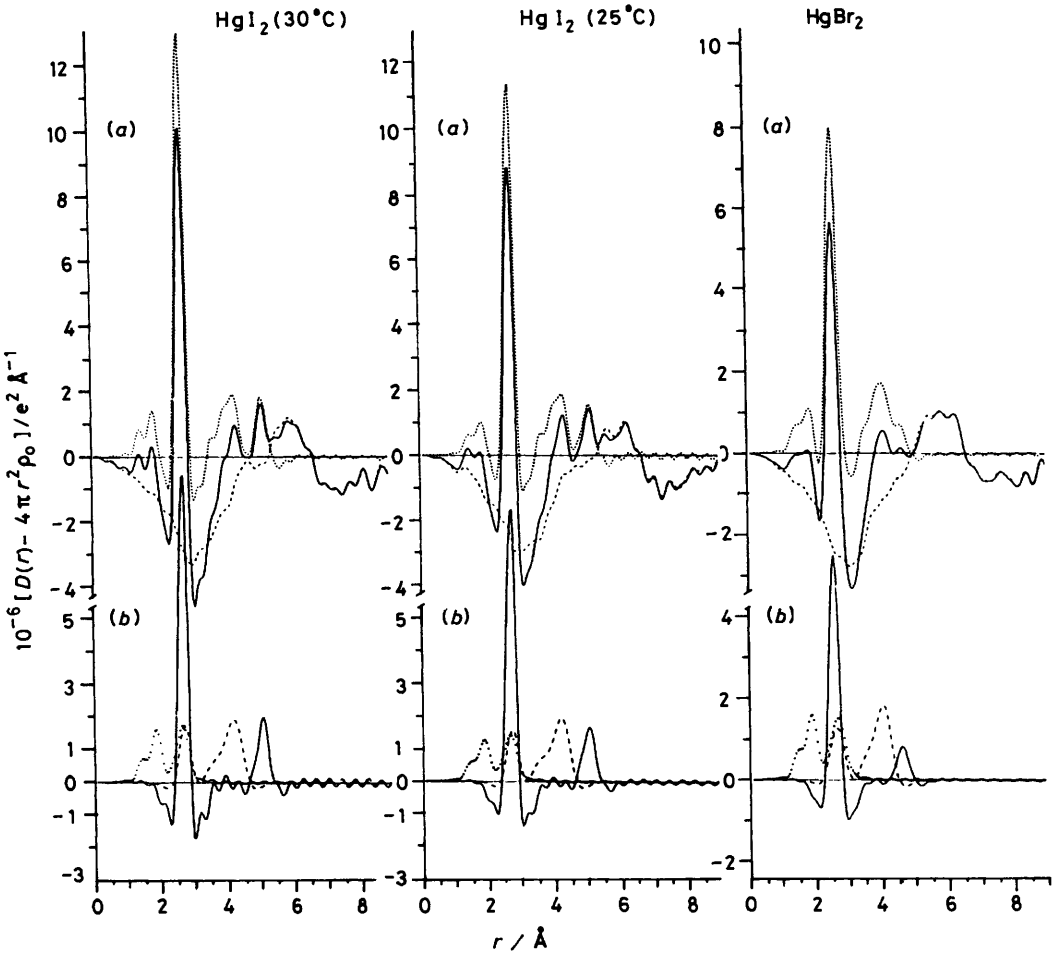

Figure 2. The $D(r) - 4\pi r^2\rho_0$ functions (r.d.f.s) and calculated peak shapes for the $[HgX_2(tht)_2]$ molecular complexes with parameters from Table 2. (*a*) Experimental r.d.f.s (solid lines), total model functions (dotted lines), and their difference (dashed curves); (*b*) model functions separated into Hg–X and X • • • X peak shapes (solid lines), remaining intramolecular interactions in Table 2 (X • • • S, Hg–S, Hg • • • C, and S • • • S) (dashed lines), and the intramolecular tht peak shapes (dotted lines)

confirm that loss of tht ligand was not occurring during measurement.

Raman spectra were recorded with a Coderg T800 or a DILOR RTI 30 triple monochromator, mainly with photon-counter detection. Excitation was with a Coherent Radiation Laboratories model 52 or INNOVA 90-5 argon-ion laser, using pre-monochromated 514.5-nm radiation. Powdered solid samples were contained in sealed capillary tubes.

Results

X-Ray Diffraction.—The major peaks in the radial distribution functions, Figure 2(*a*), are found at 2.7 and 2.5 Å for the HgI_2 and $HgBr_2$ solutions, respectively. The position and size of the peaks correspond well to the values expected for two Hg–X distances (X = I or Br), from a comparison with the corresponding dmso and pyridine solutions.[2,3] On a similar basis, the peak at 5.0 Å for the HgI_2 solutions can be ascribed to the I • • • I distance within a bent HgI_2 moiety.

In the crystal structure comprised of discrete molecules of $[HgBr_2(tht)_2]$ the Br • • • Br distance is 4.37 Å,[4] in $[HgBr_2(py)_2]$-(s) it is 4.68 Å,[10] and in a solution of $HgBr_2$ in pyridine (py) it is 4.79 Å.[2] The small peak at 4.6 Å in the r.d.f. of the $HgBr_2$ solution in tht is therefore assigned to the Br • • • Br distance in a $HgBr_2$ species. The minor peaks at 1.4 and 1.9 Å correspond to the C–C and C–S bonds within the tht molecules. The composite peaks at 4.3 and 4.1 Å in the HgI_2 and $HgBr_2$ solutions, respectively, can be related to both the X • • • S and Hg • • • C distances within an $HgX_2(tht)_2$ complex as derived from the crystal structures, see Table 2. All solutions also show two broad peaks centered around 6 and 10 Å. Similar features at about the same distances were also found in the r.d.f.s of all dmso and pyridine solutions, and originate from the intermolecular distances in the liquid.

A co-ordination model based on the crystal structures of the molecular complexes $[HgBr_2(tht)_2]$ and $[HgCl_2(tht)_2]$ (Figure 3) has been used to calculate peak shapes corresponding to intramolecular interactions within the molecular complex. The sum of the calculated peak shapes [dotted lines in Figure 2(*a*)] with parameters according to Table 2 explains all distinct short-range peaks in the r.d.f.s. The difference functions (dashed lines) are similar for all three solutions and only the previously mentioned broad features at 6 and 10 Å remain over an even background.

In Figure 2(*b*) the calculated peak shapes have been divided into different categories. The intramolecular Hg–X and X • • • X interactions are represented by dotted lines. The dominant and well defined Hg–X distances give rise to significant intensity variations in the $i(s)$ curve extending beyond the experimental limit $s_{max.} = 16.5$ Å^{-1}. The cut-off of the Fourier integration at $s_{max.}$ with the moderate damping used (see above) therefore causes oscillations around the main Hg–X peaks, but as they

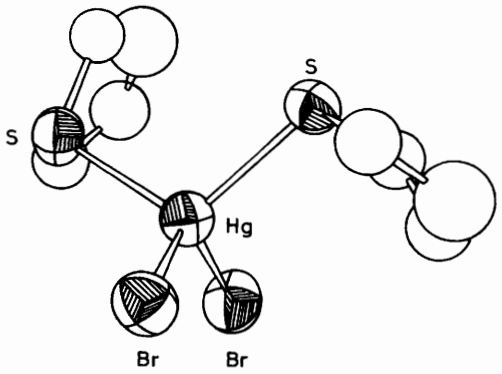

Figure 3. The crystal structure of the $[HgBr_2(tht)_2]$ molecular complex[4]

occur in the same way in the calculated and experimental curves they will cancel in a difference. The other calculated contributions from intramolecular interactions as estimated on the basis of the crystal structure distances,[4] Hg • • • C, Hg–S, X • • • S, and S • • • S, are shown by the dashed line. The Hg–S contributions are overlapped by the Hg–X peak, and the Hg • • • C and S • • • S interactions are too insignificant to be accurately determined. Only the X • • • S distances within the molecule, which are the dominant contributors to the peak just above 4 Å, can be obtained from the solution data.

The tht molecules, free and co-ordinated, have been treated as entities with fixed geometry using average values from the crystal structures.[4] The peak shapes for the tht molecules [dotted curves in Figure 2(*b*)] satisfactorily explain the peaks at 1.4 and 1.9 Å in the r.d.f.s. The C • • • C and C • • • S diagonal distances within the tht molecules, which almost coincide with the Hg–S peak, make a contribution to the Hg–X peak region at about 2.6—2.7 Å, of similar magnitude to that from the Hg–S distances (dashed line).

The parameters of the model, *i.e.* the mean distance d, its root-mean-square variation l, and the number of distances n for each interatomic interaction, have been systematically varied in order to find the best fit to the experimental curves. As the model only accounts for well defined short-range distances it cannot explain the low-angle region of the experimental intensities, but the calculated intensity curves (solid lines in Figure 1), which correspond to the peak shapes in Figure 2(*a*), explain satisfactorily the experimental $si(s)$ curves in the high-angle region $s > 4$ Å^{-1}, where the highly damped intermolecular intensity contributions can be neglected. No attempt was made to introduce an approximate model to describe the packing of the molecules in the liquid.

The calculated intensities for a pair of atoms p,q were obtained from expression (2) where f is the X-ray atomic

$$i_{calc.}(s) = (f_p f_q + \Delta f_p'' \Delta f_q'') \sin sd_{pq}/(sd_{pq})^{-1} \exp(-l^2 s^2/2) \quad (2)$$

scattering factor corrected for the real part of the anomalous dispersion and $\Delta f''$ is its imaginary part.[11] Least-squares refinements of the calculated intensities are of limited value as only a few parameters of the model will contribute sufficiently to be refined independently in the high-angle region, while the remaining ones must be held constant at assumed values. The standard deviations given in Table 2 are therefore mainly based on the variation of the fit of the peak shapes to the r.d.f.s for systematic changes in the main parameters of the model.

As discussed previously[2,3] the vibrations of the halide atoms perpendicular to the Hg–X bonds will in solution give rise to an apparent shortening of the experimental X • • • X distance of about 0.04 Å for the HgI_2 and $HgBr_2$ entities.[12] The corrected angles are given in Table 2.

Vibrational Spectra.—The main point of interest concerns Hg–X stretching vibrations. I.r. spectra of $HgBr_2$ and HgI_2 in tht show just two pronounced and well resolved bands with a marked halide dependence; in each case the higher-wavenumber feature (X = Br, 211; I, 177 cm^{-1}) is the more intense. The corresponding Raman spectra are dominated by an intense polarized band (X = Br, 179; I, 140.5 cm^{-1}) corresponding to the lower of the two i.r. bands, and which is clearly assignable as the symmetric HgX_2 stretching vibration; a shoulder corresponding to the asymmetric HgX_2 mode is more clearly visible under crossed polarization conditions. For $HgCl_2$ in tht, the i.r. spectrum shows a single broad $HgCl_2$ stretching feature as does the Raman spectrum, but the band maxima are slightly different (i.r., *ca.* 288; Raman, *ca.* 278 cm^{-1}) giving an approximate indication of the asymmetric and symmetric stretching frequencies.

The spectra of the solid bromide and iodide complexes $[HgX_2(tht)_2]$ can be readily correlated with those of the solutions. In the i.r. spectra below 400 cm^{-1} there are bands at 296, 223, 183, and 170 cm^{-1} for X = Br, and 295, 211, 157, and 133 cm^{-1} for X = I. In each case the higher two must relate to modes involving bound tht, and although they are visible in the Raman spectra they are much weaker. The two principal bands in the Raman spectra occur at 184 and 169 cm^{-1} for the bromide and at 155 and 130 cm^{-1} for the iodide compound, with the strongest band at the lower frequency. The intensity ratio for the corresponding i.r. bands is inverted which indicates that the symmetric stretching HgX mode can be assigned to the lower-frequency band.

The i.r. spectrum of the solid $[HgCl_2(tht)_2]$ complex shows four bands between 400 and 100 cm^{-1} at 314, 267, 244, and 221 cm^{-1}, all of comparable intensity. The highest and lowest of these presumably correlate with the ligand-dependent modes seen for the other halide derivatives. In the same range, the Raman spectrum shows just two prominent bands of similar intensity at 267 and 244 cm^{-1}, which we assign as HgCl stretching features. The relative intensities of the two bands in the Raman and i.r. spectra are too close to allow a conclusive assignment, but it seems possible that the asymmetric stretching frequency is higher than the symmetric one. Such an unusual order is found for example for some phosphine complexes $[HgX_2(PR_3)_2]$.[13]

Discussion

The sulphur atom in tht has a high donor capacity towards the mercury atom in the HgX_2 molecules. This is shown for example by a comparison of the stretching vibrational frequencies of HgX_2 in a large range of solvents of different properties.[1] The present data show that even when the number of available solvent molecules is large, as in a solution, the mercury atom restricts its co-ordination to pseudo-tetrahedral. For the $[HgBr_2(tht)_2]$ molecular complex, for which both solution and crystal structure data have been obtained, a notable difference is that the BrHgBr angle is significantly smaller in the crystal, 117.5(1)°, than in solution, 132(2)°. Even without corrections for thermal motion, the mean Hg–Br distance in the crystal, 2.553 Å, is longer than the solution value, 2.535(6) Å.

Both the IHgI and BrHgBr angles are smaller than in comparable dmso or pyridine solutions.[2,3] They are still considerably greater than the tetrahedral values, which is a clear indication that although the S atom of tht is a better donor towards the mercury atom than the O and N atoms of dmso and pyridine, respectively, it is clearly outranked by the I and Br ligands. For the P donor in the $[HgX_2(PPh_3)_2]$(s) complexes with X = I or Br, however, all ligands seem to have a comparable donor strength as judged from the angles. This is

Table 3. Hg–X stretching frequencies (cm^{-1}) in $[HgX_2(tht)_2]$ complexes in the crystal and in tht solution

	Solid		Solution	
Complex	sym	asym	sym	asym
$[HgCl_2(tht)_2]$	267	244	278	*ca.* 288
$[HgBr_2(tht)_2]$	169	183	179	211
$[HgI_2(tht)_2]$	130	157	140.5	177

also consistent with the longer Hg–X distances[14,15] [Hg–I 2.748 and Hg–Br 2.630(8) Å] than in the present study.

On the other hand the S atom of thioethers or alkyl sulphides can compete effectively with Cl as a ligand in adducts with $HgCl_2$. Several examples of this are found in reviews by Graddon[16] and Dean.[17] The structure of $HgCl_2$·tht, for example, has been described as a substitution complex rather than an addition compound with a zigzag ribbon of alternating $[HgCl(SC_4H_8)]^+$ and Cl^- ions.[18] This tendency to ionize may be a reason for the comparatively low solubility of $HgCl_2$ (*ca.* 0.37 mol dm^{-3} at 25 °C)[6] in tht, because the low dielectric constant ($\varepsilon \approx 8$, estimated value) of this solvent does not favour dissociation of ionic compounds.

As discussed for the mercury(II) halide solutions in pyridine,[2] solvent interaction with the halide atoms may increase the XHgX angle in solution as compared to the crystal structure. The dipole moment of tht (1.90 D $\approx 6.34 \times 10^{-30}$ C m)[19] is lower than that of pyridine (2.23 D),[20] which indicates that effects other than dipole–dipole interactions are involved in causing the large discrepancy between the BrHgBr angle of the $[HgBr_2(tht)_2]$ complex in solution and in the crystal. An obvious difference between pyridine and tht as ligands is that the S atom of tht has a free electron pair able to interact with for example another solvent molecule. Such an interaction (probably S · · · S, see below) would decrease the Hg–S bond strength and consequently decrease the Hg–Br bond length in the $[HgBr_2(tht)_2]$ species in solution, as seems to be the case. The increasing *s*-orbital content in the Hg–Br bond would then be expected to contribute to the widening of the BrHgBr angle. The comparisons in Table 3 of the vibrational spectra of the molecular $[HgX_2(tht)_2]$ species (X = I, Br, or Cl) in the crystals and in tht solutions in all cases show an increase in the stretching frequencies consistent with a stronger Hg–X bond in the solutions.

An interesting observation is that the heats of solvation and formation, $-\Delta H_{sv}^{\circ}$, of the $[HgX_2(tht)_2]$ molecular species are much higher when determined in dilute benzene solutions of tht than in pure tht, much more so than for the corresponding pyridine solutions, for example.[6] In tht the reported values are: for $HgCl_2$, 138.2 and 118.9; $HgBr_2$, 136.8 and 124.1; and HgI_2, 129.2 and 120.0 kJ mol^{-1}, respectively. Moreover, from a comparison between a number of ΔH_{sv}° values determined for a series of solvents with increasing co-ordinating ability, in particular the values for the S-donor solvents tht and dibutyl sulphide were found to deviate and be lower than expected, Table 9 of ref. 6. It was proposed that these effects are due to a more ordered bulk structure in these solvents caused by specific S · · · S interactions.[6]

A rather pronounced intermolecular liquid structure is indicated in the tht solutions by the broad peaks at about 6 and 10 Å in the r.d.f.s, but similar features are also found for pyridine solutions although with a smaller magnitude. It is not possible from the present diffraction data to distinguish between effects of preferred positions from the packing of the molecules in the liquid, and the effects caused by specific solvent–solvent interactions. It would therefore be of interest to determine the r.d.f. of pure tht in order to assess the nature of possible direct S · · · S interactions in the region 3—4 Å. In the present concentrated solutions with only about eight free tht molecules per $[HgX_2(tht)_2]$ species no distinct features of this type can be detected in this region.

Acknowledgements

We gratefully acknowledge the financial support given by the Swedish Natural Science Research Council and the S.E.R.C.

References

1 I. Persson, M. Sandström, and P. L. Goggin, *Inorg. Chim. Acta*, 1987, **129**, 183.
2 I. Persson, M. Sandström, P. L. Goggin, and A. Mosset, *J. Chem. Soc., Dalton Trans.*, 1985, 1597 and refs. therein.
3 M. Sandström, *Acta Chem. Scand., Ser. A*, 1978, **32**, 627.
4 M. Sandström and I. Persson, unpublished work.
5 F. Gaizer and G. Johansson, *Acta Chem. Scand.*, 1968, **22**, 3013.
6 I. Persson, M. Landgren, and A. Marton, *Inorg. Chim. Acta*, 1986, **116**, 135.
7 G. Johansson, *Acta Chem. Scand.*, 1966, **20**, 553; 1971, **25**, 2787.
8 M. Sandström, I. Persson, and S. Ahrland, *Acta Chem. Scand., Ser. A*, 1978, **32**, 607.
9 G. Johansson and M. Sandström, *Chem. Scr.*, 1973, **4**, 195.
10 A. J. Canty, C. L. Raston, B. W. Skelton, and A. W. White, *J. Chem. Soc., Dalton Trans.*, 1982, 15.
11 'International Tables for *X*-Ray Crystallography,' Kynoch Press, Birmingham, 1974, vol. 4.
12 S. J. Cyvin, 'Molecular Vibrations and Mean Square Amplitudes,' Elsevier, Amsterdam, 1968, p. 311.
13 N. A. Bell, T. D. Dee, P. L. Goggin, M. Goldstein, R. J. Goodfellow, T. Jones, K. Kessler, D. M. McEwan, and I. W. Nowell, *J. Chem. Res*, 1981, (*S*) 2.
14 L. Fälth, *Chem. Scr.*, 1976, **9**, 71.
15 N. A. Bell, T. D. Dee, M. Goldstein, P. J. McKenna, and J. W. Nowell, *Inorg. Chim. Acta*, 1983, **71**, 135.
16 D. P. Graddon, *Rev. Inorg. Chem.*, 1982, **4**, 211.
17 P. A. W. Dean, *Prog. Inorg. Chem.*, 1978, **24**, 109.
18 C-I. Bränden, *Ark. Kemi*, 1964, **22**, 495.
19 C. W. N. Cumper and A. I. Vogel, *J. Chem. Soc.*, 1959, 3521.
20 L. E. Orgel, T. L. Cottrel, W. Dick, and L. E. Sutton, *Trans. Faraday Soc.*, 1951, **47**, 113.

Received 21*st July* 1986; *Paper* 6/1463